# Rescue of the endogenous FVIII expression in hemophilia A mice using CRISPR-Cas9 mRNA LNPs

Chun-Yu Chen,[1] Xiaohe Cai,[1] Barbara A. Konkle,[2,3] and Carol H. Miao[1,4]

[1]Seattle Children's Research Institute, Seattle, WA 98101, USA; [2]Washington Center for Bleeding Disorders, Seattle, WA 98101, USA; [3]Department of Medicine, University of Washington, Seattle, WA 98195, USA; [4]Department of Pediatrics, University of Washington, Seattle, WA 98195, USA

**Gene editing provides a promising alternative approach that may achieve long-term FVIII expression for hemophilia A (HemA) treatment. In this study, we investigated *in vivo* correction of a mutant factor VIII (FVIII) gene in HemA mice. We first developed MC3-based LNPs for efficient mRNA delivery into liver sinusoidal endothelial cells (LSECs), the major site of FVIII biosynthesis. To target a five base pair deletion in FVIII exon 1 in a specific HemA mouse strain, we injected LNPs encapsulating Cas9 mRNA and specifically designed sgRNAs intravenously for *in vivo* gene editing of the mutant FVIII. Indel variants generated at the mutant site contained mostly a single base-pair deletion, resulting in frameshift correction of FVIII gene. Sustained endogenous FVIII activity up to 6% was achieved over 26 weeks in treated HemA mice. Sequencing data indicated an average gene editing rate of 15.3% in LSECs. Our study suggests that optimized MC3 LNP formulations, combined with CRISPR-Cas9 technology, can effectively correct the mutant FVIII gene in LSECs and restore FVIII activity for therapeutic treatment of HemA.**

## INTRODUCTION

Hemophilia A (HemA) is a bleeding disorder caused by a deficiency of factor VIII (FVIII) due to a variant in the *F8* gene on the X chromosome. The severity of HemA depends on the residual FVIII activity, which can result in a range of symptoms from mild to severe. Patients with severe HemA exhibit less than 1% of FVIII activity and are prone to prolonged bleeding after trauma, as well as spontaneous bleeding in soft tissues such as joints and muscles.[1,2] Current treatment options, such as frequent infusions of therapeutic recombinant FVIII protein to maintain FVIII activity above the normal trough level of >1% are expensive, inconvenient, short-term, and frequently insufficient. Gene therapy is an emerging field that offers great promise as an alternative method to treat HemA patients. Most current gene therapy trials for HemA aim to introduce the FVIII gene into hepatocytes using adeno-associated viral (AAV) vectors. Although recent clinical trials using AAV vectors have yielded promising results, pre-existing immune response against AAV can diminish the efficacy of gene therapy and repeated administration of treatment is currently impossible in patients with pre-existing anti-AAV antibodies.[3,4]

Direct correction of the mutant *F8* gene in HemA patients can result in long-term improvement of symptoms, making it a promising alternative to gene replacement therapy. A precise gene editing method developed recently involves clustered regularly interspaced short palindromic repeats (CRISPR) that utilizes CRISPR-associated endonuclease 9 (Cas9) and single guide RNA (sgRNA) to induce double-strand break (DSB) in specific DNA sequences.[5] This technique triggers the error-prone DSB repair mechanism including non-homologous end-joining (NHEJ), which introduces insertion-deletion mutations (indels) at the targeting site. By inducing indels, it is possible to alter the reading frame, enabling not only gene knockout but also correction of diseases caused by frameshift variants via indel-mediated repair.[6] This powerful gene editing tool is effective in both *in vitro* and *in vivo* systems.

Lipid nanoparticles (LNPs) offer a promising nonviral approach for gene therapy, as they can efficiently transport nucleic acids (mRNA, DNA, and siRNA) to targeted organs or cell types while protecting them from degradation.[7,8] Using mRNA encapsulated LNPs to deliver gene editing tools offers several advantages, including the short half-life of mRNA that allows for rapid and transient gene editing while preventing off-target effects resulting from prolonged Cas9 expression by plasmid or viral vector. Additionally, unlike DNA, mRNA does not pose a risk of oncogenic mutagenesis via insertion into the genome. Previous studies have successfully utilized LNPs to deliver therapeutic siRNA or mRNA for treating various diseases.[9] In fact, the first Food and Drug Administration (FDA)-approved LNP drug, Onpattro, which contains small interfering RAN (siRNA), was authorized for the treatment of hereditary ATTR amyloidosis in 2018.[10,11] More recently, mRNA LNPs encoding the viral spike protein have been authorized as vaccines to prevent SARS-CoV-2 (COVID-19) infection.[12,13] Upon systemic injection, LNPs are known to preferentially accumulate in the liver due to its high blood perfusion rate to take up the majority of circulating lipids. The serum

apolipoprotein E (ApoE) on the surface of the LNPs contributes to their preferential targeting of hepatocytes that express low-density lipoprotein (LDL) receptors.[14,15] Previous studies have demonstrated that routine administration of FVIII mRNA encapsulated in LNPs significantly enhances clotting activity in Hem A mice, which is more effective than FVIII protein replacement therapy.[16] Additionally, the delivery of anti-CD3 antibody mRNA encapsulated in LNPs, following FVIII gene therapy, has been shown to reduce the immune response against FVIII, which affects 30% of HemA patients receiving protein replacement therapy.[17] However, achieving long-term therapeutic effect via LNP delivery of FVIII mRNA remains challenging. Alternatively, a nonviral *in vivo* gene editing approach can provide permanent correction of the *F8* gene that is regulated in its native site. Liver sinusoidal endothelial cells (LSECs) are the primary source of FVIII synthesis.[18] They play a significant role in the scavenging system of the liver and have the highest endocytic ability. This high endocytic ability, coupled with their contribution to FVIII production, makes LSECs an attractive target for gene editing strategies aimed at restoring functional FVIII levels in HemA patients. Thus, identifying appropriate vehicles for gene delivery into LSECs is essential for developing more effective and lasting HemA treatments.

In this study, we synthesized D-Lin-MC3-DMA (MC3)-based LNPs encapsulating reporter mRNAs and verified their biodistribution in LSECs. Additionally, we successfully delivered Cas9 mRNA and sgRNA using LNPs to induce indel mutations in the mutant *F8* gene and correct the associated nonsense mutation in HemA mice. The treated mice exhibited indel repair at the mutant site and restoration of endogenous plasma FVIII activity *in vivo*. This restored FVIII activity was sustained for over 26 weeks, resulting in improved function of clot formation in HemA mice.

## RESULTS

### Synthesis and optimization of LNP formulations

In this study, we synthesized mRNA LNPs using ionizable cationic lipids, specifically MC3, which is the same lipid used in the first FDA-approved LNP-based RNA interference (RNAi) drug.[10,11] Ionizable cationic lipids exhibit positive charges in low pH environments and can therefore bind to the negative charges of phosphate backbones in nucleic acids such as mRNA, siRNA, and DNA. At physiological pH 7.4, only a portion of the amides in ionizable lipid remains protonated, leading to a weak negative surface, which can reduce the cell toxicity.[19,20] In addition, the positive charge of ionizable lipids enables the nucleic acids to be released from the endosome by binding to the negatively charged endosomal membrane. Cationic lipid is the most important component in LNPs, as it determines the potency of LNPs. LNPs composed of MC3 cationic lipids have been reported to have liver-targeting ability after systemic delivery.[21,22] Besides ionizable cationic lipid, the ratio between other lipid components, including cholesterol, helper lipid and lipid-conjugated polyethylene glycol (PEG) is also important. We incorporated the helper lipid DOPE and DMG-PEG$_{2000}$ into MC3 LNP formulation to facilitate and stabilize the formation of LNPs. Cholesterol was

also used to enhance LNP stability and help LNP escape from endosome.

To optimize LNP formulation, we synthesized the luciferase mRNA encapsulated MC3 LNP (Luc LNP). We used a microfluidic system, NanoAssemblr Benchtop, to mix the luciferase mRNA aqueous phase with the lipid ethanol phase containing MC3, cholesterol, DOPE, and DMG-PEG$_{2000}$ at ratios of 50:10:39:1, respectively. After synthesis of the LNP, all the materials were diluted with PBS (pH 7.4) and concentrated to an appropriate volume by Amicon centrifugal filter. Since the charge ratio between nitrogen group of cationic lipid and phosphate group of nucleic acid significantly affects encapsulation efficiency and size,[23,24] we optimized the Luc LNPs according to N/P ratio of 3–8. Results showed that a higher N/P ratio allowed for enhanced encapsulation efficiency and *in vivo* transfection efficiency (Figures 1A–1C). Since the N/P of 8 resulted in a higher yield compared with N/P of 6 (61.7% vs. 47.5%), we selected N/P 8 for the following experiments. The size of the formulated LNPs was validated prior to injection (Figures 1D and 1E). The mean particle size of LNPs was approximately 163 nm. We assessed potential liver damage by evaluating plasma transaminase levels in mice treated with 1 mg/kg Luc LNPs. None of the treated mice showed elevated alanine aminotransferase (ALT) and aspartate aminotransferase (AST) levels compared with the untreated mice (Figures 1F and 1G). These data suggested that treatment with a high dose of MC3 LNP did not induce any significant liver damage, indicating that MC3 LNPs are suitable for *in vivo* treatment.

### Biodistribution of MC3 LNPs

To investigate the liver distribution of MC3 LNP, we intravenously injected 1,1′-Dioctadecyl-3,3,3′,3′-tetramethylindocarbocyanine perchlorate (DiI)-labeled LNPs (0.4 mg/kg) into mice. DiI is a lipophilic dye that can diffuse and target cells. One hour after injection, mouse livers were harvested and stained with FITC-Isolectin B4 as a vascular stain after cryosection to confirm the *in vivo* distribution. The staining images revealed that most of DiI-labeled liver cells were hepatocytes. Interestingly, DiI-labeled cells also colocalized with Isolectin B4-labeled LSECs suggesting that LNPs have LSEC-targeting ability (Figure 2A). To further confirm the targeting specificity and efficiency, we encapsulated GFP mRNA into LNPs (GFP LNP) and intravenously injected them into mice at a dosage of 1.2 mg/kg. Six hours after injection, we euthanized the treated mice and collected their livers to perform immunostaining. We used lymphatic vessel endothelial hyaluronan receptor-1 (LYVE-1) as a marker for LSECs. The immunostaining images showed colocalization of LYVE-1 and GFP signals, indicating that LSECs not only uptake LNPs but can also express GFP protein (Figure 2B). Next, we used Luc LNPs to evaluate mRNA expression levels in hepatocytes and LSECs, respectively. Livers of the treated mice were perfused, and the harvested cells were centrifuged to separate parenchymal (hepatocytes) and non-parenchymal cells. We further isolated LSECs from non-parenchymal fraction using anti-CD146 beads. The purified cells were stained with the endothelial cell marker, anti-CD31 antibody to confirm their LSEC lineage specificity (Figure S1). Luciferase activity was examined using *in vitro* luciferase assay
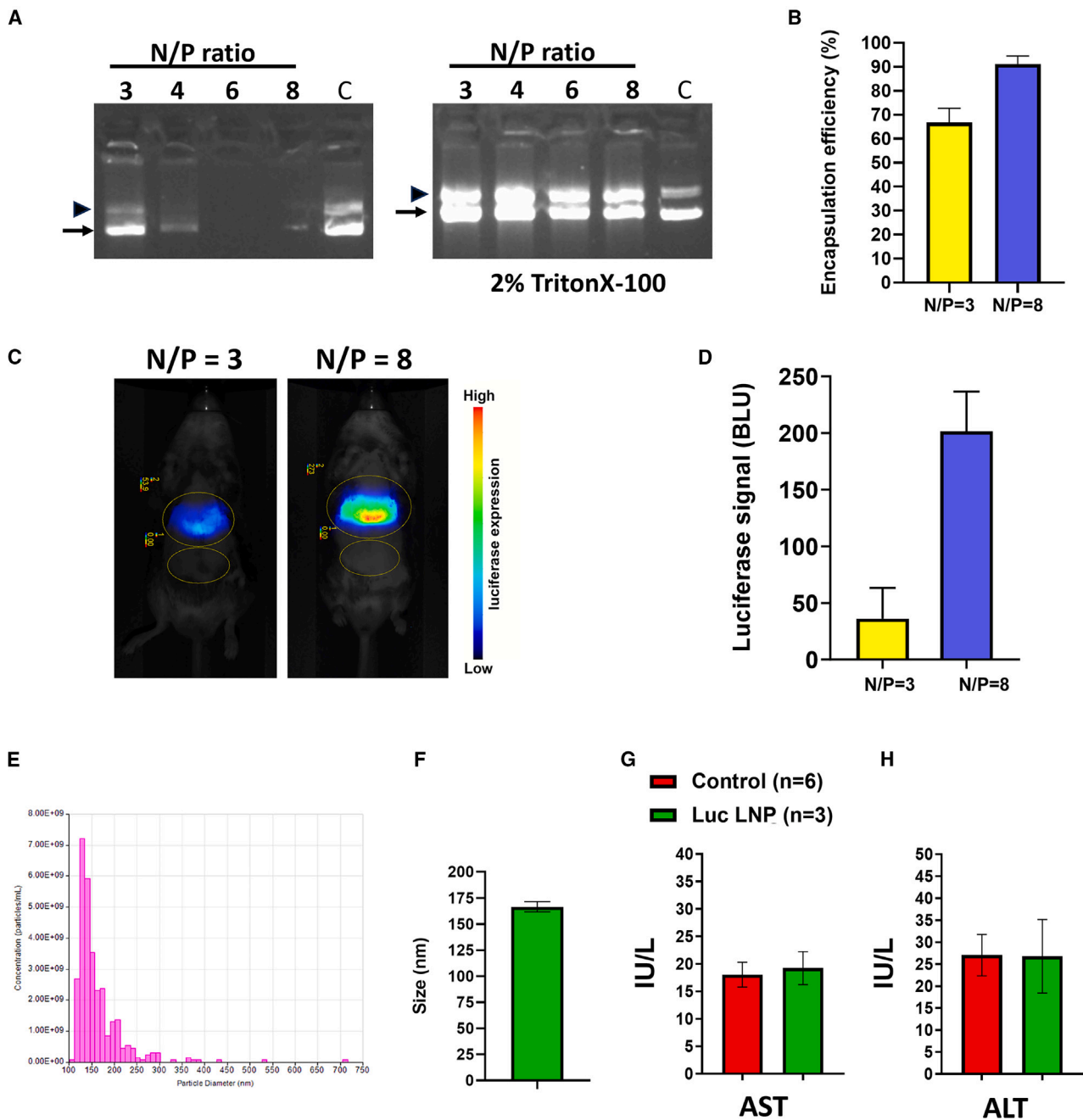
**Figure 1. Optimization of MC3 lipid nanoparticles**

(A) Gel electrophoresis analysis of MC3 lipid nanoparticles (LNPs) at different N/P ratios. Arrowheads and arrows indicate nicked form and supercoiled form of double-strand DNA, respectively. (B) Encapsulation efficiency of luciferase mRNA LNP (Luc LNP) at N/P ratios of 3 and 8, determined by RiboGreen assay.

(C) Evaluation of luciferase expression 6 h after intravenous injection of 0.3 mg/kg Luc LNPs at N/P ratios of 3 and 8 using IVIS imaging. (D) Quantification of luciferase expression from IVIS imaging, presented as mean luciferase signals ± standard deviations, expressed in bioluminescence light units (BLUs), N/P 3, $n = 3$; N/P 8, $n = 6$. Characterization of LNP: (E) size distribution and (F) average size at N/P ratio = 8 was analyzed using qNano. Examination of plasma (G) AST and (H) ALT levels 1 day after intravenous injection of 1 mg/kg Luc LNP.
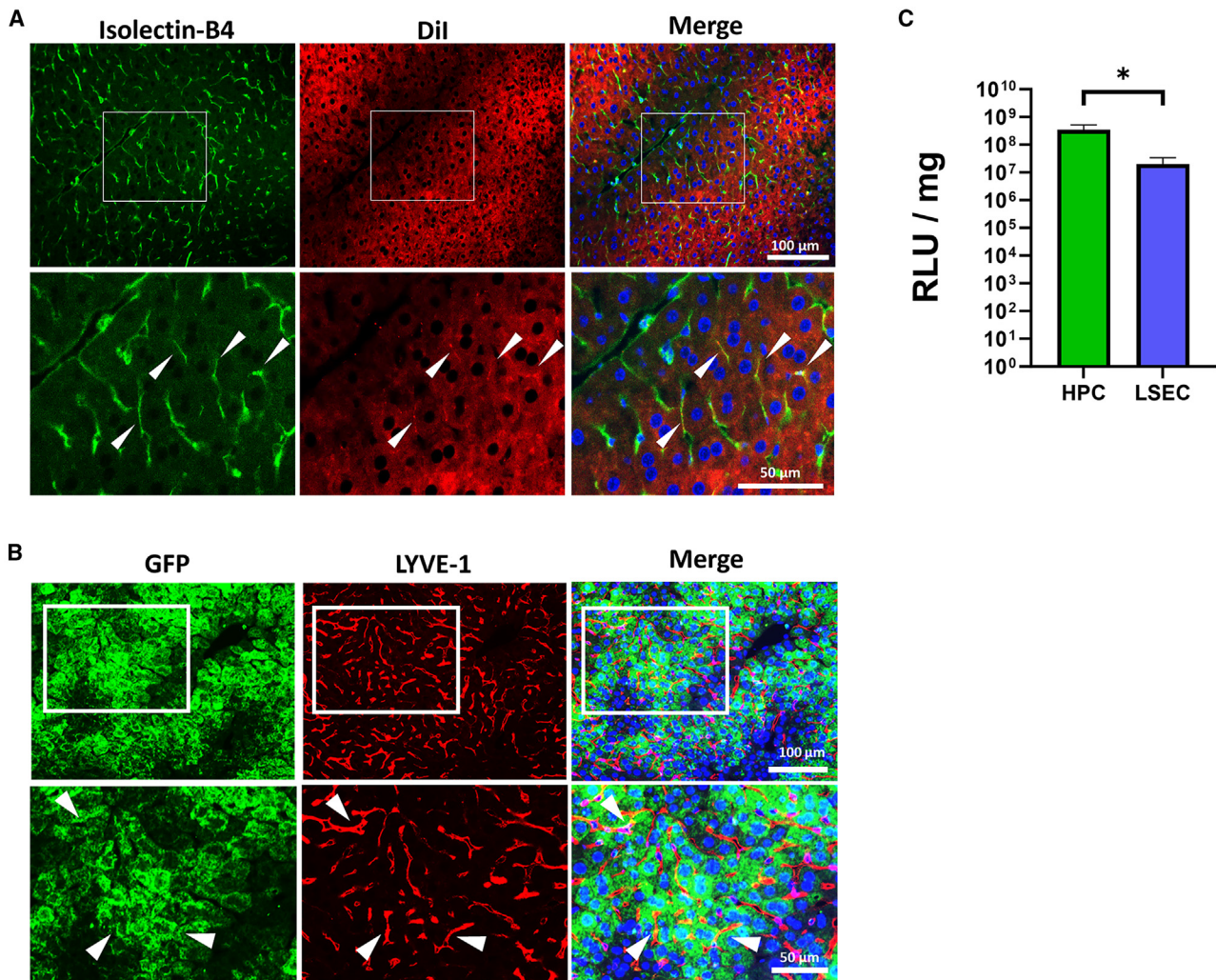
**Figure 2. Cell distribution of MC3 LNPs after intravenous injection in mice**

(A) One hour after intravenous injection of DiI-labeled LNPs (red) in mice, liver tissues were harvested and stained with FITC-Isolectin-B4 (green) to mark vascular cells. Colocalization of LNPs and vascular cells were indicated by white arrowheads. (B) To determine the LSEC-targeting ability, mice were intravenously injected with 1.2 mg/kg of GFP LNPs. Liver sections harvested 6 h after LNP injection were stained with anti-GFP (green) and anti-LYVE-1(red) antibodies. Co-stained cells were highlighted using white arrowheads. Enlarged images of the staining within white squares are presented below. (C) Mice were treated with 0.2 mg/kg Luc LNPs. Livers of treated mice were perfused with Liberase to obtain single cell suspensions. The total liver cells were subsequently purified to isolate hepatocytes (HPCs) and LSECs. Luciferase expression of HPCs and LSECs were determined by luciferase assay and normalized by total protein, respectively. Data are presented as average experimental values ± standard deviation.

(Figure 2C). The results indicated that high levels of luciferase expression were obtained from both hepatocytes and LSECs with about 17-fold higher expression in hepatocytes than LSECs. These data indicate MC3 LNPs can efficiently transfect both hepatocytes and LSECs.

**Animal model for *in vivo* gene editing**

To assess the *in vivo* gene editing efficacy, we established a colony of hemophilia A mouse model on an immunodeficient NOD.Cg-Prkdc$^{scid}$ Il2rg$^{tm1Wjl}$/SzJ mice (NSG) background (NSG HemA). The mice carry a five base-pair deletion in mouse exon 1, leading to a premature stop codon (Figure 3A) with only 37 amino acids being

translated. Since LSECs are the primary source of plasma FVIII protein, our aim was to induce an indel mutation into the mutant mouse FVIII gene in LSECs to corrects the reading frame. Either insertion or deletion that rescues the reading frame from the nonsense variant can help restore expression of the endogenous mouse *F*8 gene. To achieve this, we designed two different sgRNAs for Cas9 nuclease targeting the mutant mouse *F*8 gene. One of these sgRNAs, mF8sgRNA, can target both wild-type (WT) *F*8 gene and mutant *F*8 gene in NSG HemA mice (Figure 3A), while the other, NSGHAsgRNA specifically targets the mutant FVIII gene in NSG HemA mice. We separately delivered Cas9 protein with these two sgRNAs to mouse fibroblast NIH3T3cells. The genomic DNA was extracted from the cells
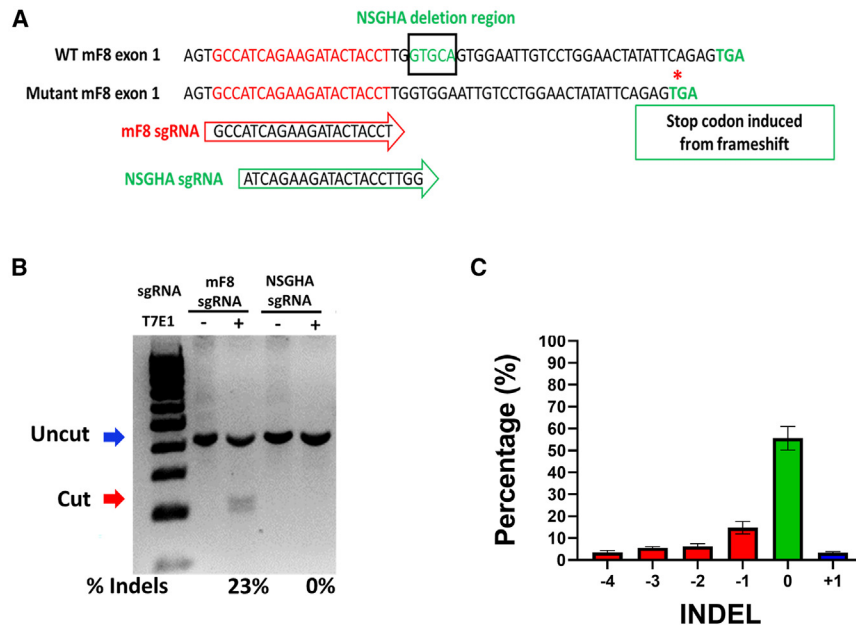
**Figure 3. *In vitro* gene editing efficiency of two sgRNAs in mouse fibroblast NIH3T3cells**

(A) Representative genomic DNA sequence of wild-type (WT) and mutant mouse *F8* (mF8). Two sgRNA sequences against mutant mF8 are shown within red and green arrows. The sequence in the black square represents the deleted sequence in mutant mF8. Premature Stop codon resulted from frameshift mutation in mutant mF8 was labeled by an asterisk. (B) *In vitro* gene editing efficiency of two sgRNAs in NIH3T3cells was determined by T7 endonuclease 1 (T7E1) assay, respectively. Blue arrow represents uncut DNA and red arrow represents cut DNA. (C) The pattern of indel mutations after mF8sgRNA-mediated gene editing in NIH3T3cells was analyzed by online genomic DNA analysis tool TIDE. Data are presented as average experimental values ± standard deviation.

3 days after transfection to estimate overall gene editing efficiency using T7 endonuclease (T7E1) assay. The result indicated that mF8sgRNA could induce an indel variant into mouse *F8* exon 1 with a 23% of indel mutation rate (Figure 3B). We subsequently identified the indel pattern at the mutation site via the Sanger sequencing and Tracking of indels by Decomposition (TIDE) online tool, showing insertion and deletion rates of 3.5% and 28.5%, respectively. Among all the deletion patterns, approximately 60% were one base-pair deletions that can restore the 5′ base-pair deletion to normal reading frame (Figure 3C). As expected, NSGHAsgRNA showed no editing activity in WT *F8* gene.

**Evaluation of *in vivo* gene editing of mutant *F8* in HemA NSG mouse model**

It was previously demonstrated in our lab that following hydrodynamic injection of plasmid DNA, transfection occurred predominantly in hepatocytes; however, lower transgene expression was also observed in LSECs. Therefore, as a preliminary test to assess the *in vivo* gene editing efficacy of NSGHAsgRNA on mutant *F8*, we first employed hydrodynamic injection to deliver a co-expressing plasmid encoding Cas9 and NSGHAsgRNA into NSG HemA mice to correct the five base-pair deletion in exon 1 of the *F8* gene. Following injection, we measured endogenous FVIII activity in the treated mice using activated partial thromboplastin time (aPTT) assay. Our results indicated that delivery of Cas9/NSGHAsgRNA plasmid led to an increase in FVIII activity in NSG HemA mice. Specifically, after two injections, treated NSG HemA mice displayed approximately 2.6% FVIII activity (Figure 4A). To further assess the *in vivo* gene editing efficacy of two sgRNAs, we separately delivered plasmids encoding Cas9 and either NSGHAsgRNA or mF8sgRNA. Following injection, we euthanized the treated mice and extracted genomic DNA

from their liver tissue. We then amplified and sequenced the mutant mouse *F8* exon 1 region to determine the extent of gene editing. Our data showed that the *in vivo* gene editing efficiency of NSGHAsgRNA was comparable to that of mF8sgRNA, with both sgRNAs resulting in a gene editing efficiency of around 5% in genomic DNA extracted from whole liver (Figure 4B).

**Sustained expression of mouse FVIII following Cas9/sgRNA LNP injection**

In the last section, we demonstrated two sgRNAs exhibited similar *in vivo* gene editing efficacy through hydrodynamic injection. Following these results, we selected NSGHAsgRNA for subsequent gene editing experiments via LNP-mediated delivery of Cas9 mRNA/sgRNA. The NSGHAsgRNA was encapsulated with Cas9 mRNA into MC3 LNP and intravenously injected into NSG HemA mice at a dosage of 4 mg/kg of Cas9/sgRNA LNP. Post-treatment, FVIII activity was measured by aPTT, and our results indicated that the treated mice generated an average of 3.30% ± 0.68% of FVIII activity over a span of 26 weeks (Figure 5A). To further validate endogenous FVIII restoration, we performed rotational thromboelastometry (ROTEM) assay to monitor the clot formation using fresh whole blood collected from treated mice. Clotting time (CT) is the time when the clotting starts, and clot formation time (CFT) is the time when the clot firmness of 20 mm is detected. Results indicated that Cas9/sgRNA LNP-treated mice exhibited shorter CT and CFT durations compared with untreated mice, displaying a clotting ability better than controls containing 1% of normal whole blood. This result suggested an improved coagulation due to targeted correction of the mutant *F8* gene (Figures 5B and 5C).

We further analyzed genomic DNA from treated mice using deep sequencing to identify the gene editing rate. Administration of Cas9/NSGHAsgRNA LNP resulted in a gene editing rate of about 52.7% in total liver cells. We further isolated hepatocytes and
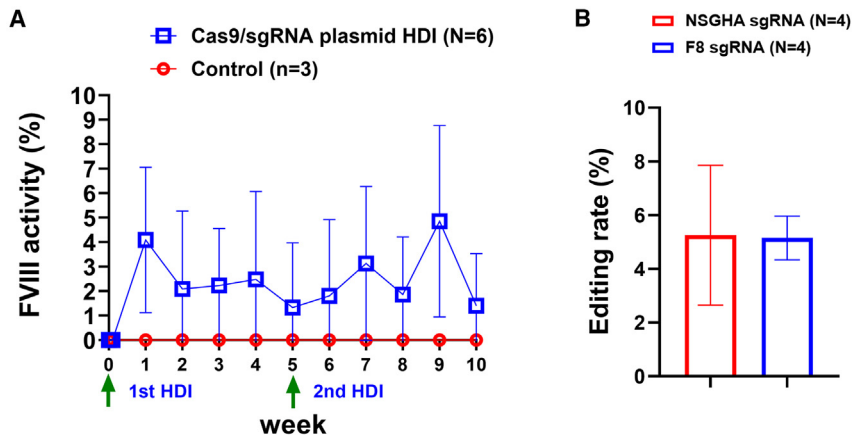
**Figure 4. *In vivo* gene editing efficiency of two specific Cas9/sgRNAs using hydrodynamic injection in NSG HemA mice**

(A) Plasmid expressing Cas9 and NSGHAsgRNA was delivered to NSG HemA mice through hydrodynamic injection. FVIII activity was evaluated by aPTT assay. Arrows indicate the injection days. (B) After hydrodynamic injection of Cas9/NSGHAsgRNA and Cas9/mF8sgRNA expression plasmid, the *in vivo* gene editing rate was analyzed by online genomic DNA analysis tool TIDE, respectively. Data are presented as average experimental values ± standard deviation.

LSECs to identify the respective gene editing rate. The data indicated that the *F8* gene was edited in 60.54% ± 11.65% of hepatocytes, whereas LSECs showed gene editing rates of approximately 16.50% ± 2.96% (Figure 6A; Table S1). No indel variants were found at five top predicted potential off-target sites when compared with untreated mice using next generation sequencing (NGS) analysis (Figure 6B). The investigation of gene editing patterns in LSECs revealed that one base-pair deletions constitute the highest editing pattern (around 46.5% of total deletions), together with four base-pair deletions, which can help rescue the five base-pair deletion in NSG HemA, accounting for 50%–60% of all the deletions (Figures 6C and 6D). We also analyzed the +2 and +5 insertion patterns among indel variants, but their frequencies were significantly lower (0.78% and 0%, respectively) compared with deletion variants (Table S2). These results suggested that Cas9/sgRNA LNP treatment induced indel repair in LSECs and restoration of the endogenous FVIII expression permanently in NSG HemA mice.

## DISCUSSION

LSECs are the primary source of FVIII biosynthesis. Previous research of LNP-mediated gene delivery has primarily focused on the hepatocyte-targeting capability of MC3-based and other LNPs to correct hepatocyte-related diseases.[25,26] While the Fah mutant mouse model has been commonly utilized to demonstrate *in vivo* gene editing efficacy in hepatocytes, there is a lack of reported studies on LSEC-related disease genes for *in vivo* gene editing experiments.[27,28] In this study, we optimized MC3 LNPs with various N/P ratio and demonstrated their ability to target different cell types *in vivo* including hepatocytes and LSECs. Our results align with previous findings, confirming the LSEC-targeting potential of MC3-based LNPs.[22] To demonstrate the *in vivo* gene editing capacity of LSECs in a disease model, we utilized a novel NSG HemA mouse model characterized by a five base-pair deletion in *F8* exon 1. Unlike conventional HemA mouse models featuring disruption of *F8* exon 16 by insertion of a *neo* cassette, this NSG HemA model presents a specific target for gene editing to restore FVIII expression by inducing indel mutations of *F8* gene in LSECs. This model mimics the genetic variant seen in approximately 16% of severe HemA patients with

small deletion and insertion variants.[29] To edit the mutant *F8* gene in NSG HemA mice, we selected two sgRNAs, mF8sgRNA and NSGHAsgRNA, targeting the mutant *F8* sequence. Since both sgRNAs exhibit similar gene editing efficiencies and to avoid repeated targeting of the corrected *F8* gene by mF8sgRNA, which also targets the WT *F8* gene, we chose NSGHAsgRNA for the subsequent gene editing experiments. Based on our findings, we successfully employed LNPs to deliver Cas9 mRNA and sgRNA to LSECs. The indel variants were generated at the deletion site to facilitate the repair of the frameshift variants in the mutant *F8* gene *in vivo*. The corrected mutant*s* exhibited endogenous FVIII expression and effectively restored the coagulation activity in NSG HemA mice. NGS sequencing analysis revealed an approximately 16.5% deletion frequency in LSECs following Cas9/sgRNA LNP treatment. Of the deletions, −1 (7.68%) and −4 (1.38%) deletion were able to restore the reading frame, potentially aiding in the recovery of FVIII expression. While +2 and +5 insertions can also restore the reading frame, <1% insertion frequency was observed. In addition, we did not detect indel variants at five top predicted potential off-target sites. The off-target effect should be carefully examined when other FVIII variants will be repaired using the indel correction strategy. With improvements in editing efficiencies, effective levels to prevent bleeding in patients with hemophilia A could be achieved. This indel repair strategy can be applied to HemA patients with frameshift mutations, in particular, for patients whose reading frames can be rescued by a one base-pair deletion using gene editing.

The advantage of *in situ* correction of mutant *F8* in LSECs is the restoration of its original and physiological function. FVIII is an acute phase protein, and its transcriptional regulation responds to various physiological conditions, such as infection, surgery, pregnancy, and inflammatory states.[30–33] Additionally, the release of FVIII occurs following acute exercise and increases during the recovery period in both healthy individuals and mild-moderate HemA patients.[34–37] Additionally, it offers great benefit to restore *F8* gene expression via gene editing in LSECs, where it undergoes unique post-translational modifications, storage, and secretion.[38] Ectopic expression of FVIII in hepatocytes, which have different post-translational modification processes than LSECs, may impact protein folding, trafficking, and release, leading to endoplasmic reticulum (ER) stress.[25,39,40] In
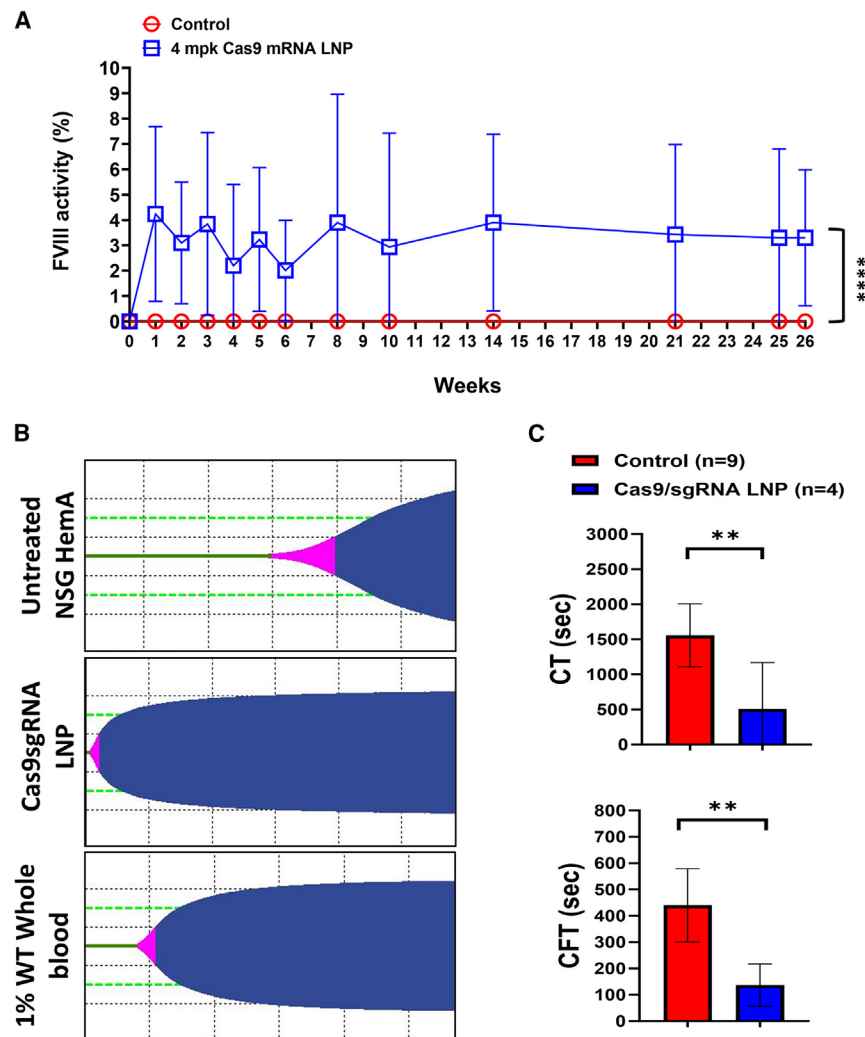
**Figure 5. Recovery of endogenous FVIII activity after Cas9/sgRNA LNP injection**

(A) FVIII activity following Cas9/sgRNA LNP treatment. NSG HemA were injected with 4 mg/kg of Cas9/NSGHAsgRNA LNP ($n$ = 2–8) to correct the mutant $F8$ gene. FVIII activity was measured by aPTT assay. The effect of LNP treatment showed significant improvement of FVIII activity. $(F_{1,95})$ = 28.14, $p$ < 0.0001. (B) NSG HemAs were treated with 4 mg/kg of Cas9/NSGHAsgRNA LNPs. Representative ROTEM graphs of coagulation activities are shown. Negative control (untreated NSG HemA) and positive controls (1% WT whole blood added to NSG HemA whole blood) were included. (C) Clotting time (CT) and clot formation time (CFT) of untreated negative control and Cas9/NSGHAsgRNA LNP-treated mice are shown. Data are presented as average experimental values ±standard deviation. Statistical comparisons were performed using two-way ANOVA in (A) and t test in (C). $**p$ < 0.01, $****p$ < 0.0001.

can sustain long-term FVIII expression and induce immunotolerance.[51,52] These factors highlight the potential benefits of utilizing LSECs as a target for $F8$ gene repair to promote effective and immune-tolerant gene therapy for HemA.

Currently, HemA gene therapy primarily relies on AAV viral vector-based gene therapy. Patients undergoing this treatment achieved a high level of FVIII expression initially; however, the FVIII expression decreases year over year after treatment.[53] Some treated patients need to revert back to prophylactic protein replacement therapy.[54] Furthermore, both pre-existing anti-AAV antibodies and newly generated antibodies following gene therapy restrict the potential for multiple treatments with AAV gene therapy. It is essential to carefully evaluate various limitations associated with this approach in HemA treatment.

On the other hand, LNP-based gene therapy offers several distinct advantages. First, LNPs exhibit low immunogenicity, enabling the possibility of repeated treatments without significant immune responses.[16,55,56] Second, the delivery of mRNA-based CRISPR-Cas9 gene editing via LNPs ensures transient expression of Cas9, thereby mitigating the risk of prolonged Cas9 presence that could otherwise trigger immune responses against Cas9-expressing cells and lead to their elimination by the immune system. Third, mRNA-based therapy eliminates the risk of oncogenic mutagenesis, as mRNA remains in the cytoplasm and does not integrate into host genome. This contrasts with viral vector-based gene therapy, where the integration of vector DNA fragments into genomic DNA poses a heightened risk

addition, von Willebrand factor (VWF) plays a crucial role as an FVIII carrier protein, preventing premature clearance and proteolytic degradation of FVIII.[41] VWF is mainly produced in capillary endothelial cells and also expressed in LSECs.[38,42] Evidence suggests that VWF can influence FVIII biosynthesis by affecting intracellular trafficking in endothelial cells and may mitigate the immune response to FVIII in the presence of anti-FVIII antibodies.[43,44] VWF is stored in Weibel-Palade bodies, and it has been observed that FVIII can be systematically or locally released along with VWF upon physiological or pharmacological stimulation.[38,45–47] However, when using hepatocytes to produce FVIII, the protein is solely localized in the cytoplasm without the accompaniment of VWF, and the controlled release of stored FVIII, as seen in LSECs, may not be achieved. Furthermore, LSECs play a crucial role as organ-resident antigen-presenting cells capable of inducing tolerance.[48] They contribute to the establishment of hepatic tolerance through the induction of regulatory T-cells (Tregs).[49,50] Studies have demonstrated that FVIII expression controlled by an LSEC-specific promoter or the $F8$ naive promoter
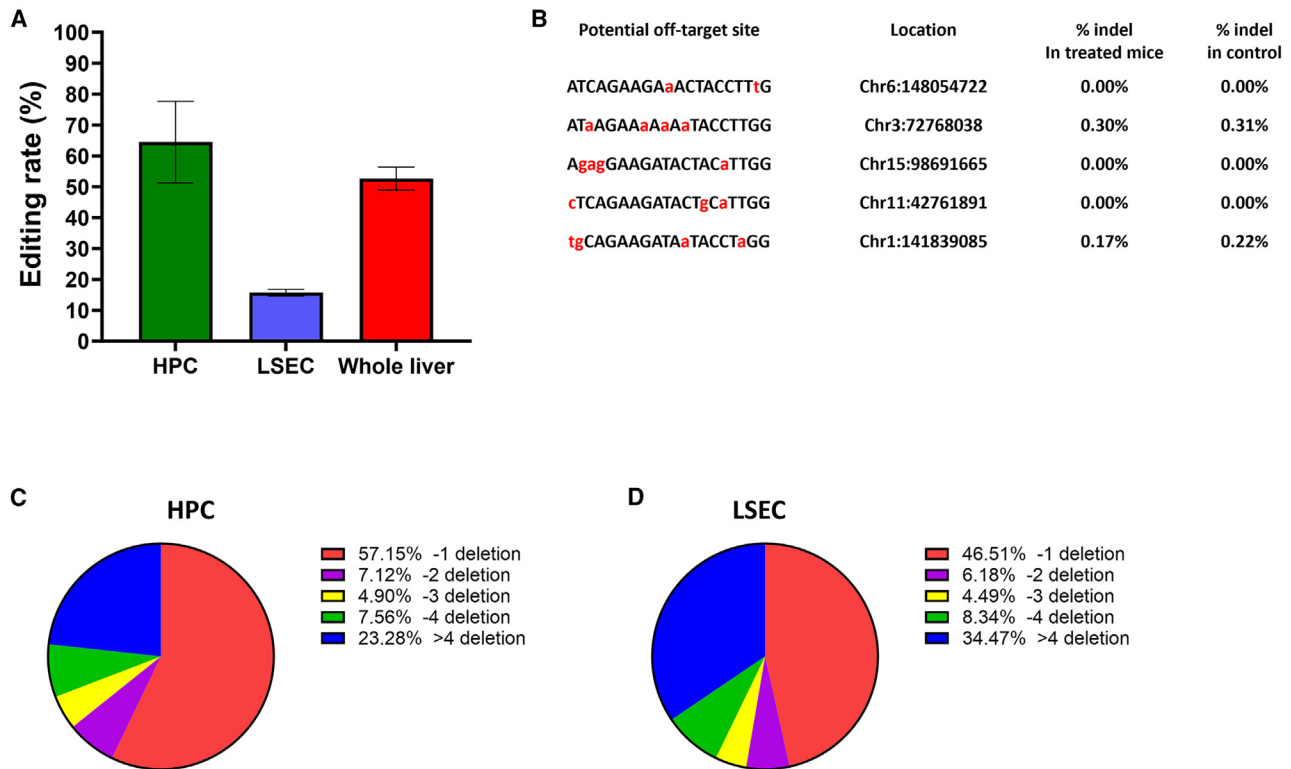
**Figure 6. Gene editing efficiency of isolated HPCs and LSECs**

After Cas9/sgRNA LNP injection, HPCs and LSECs were isolated from treated NSG HemA mice, respectively. (A) Gene editing rate of Cas9/NSGHAsgRNA from genomic DNA of whole liver, isolated HPCs and LSECs were evaluated by deep sequencing, respectively ($n = 3$). (B) Indel frequencies at five top predicted potential off-target sites were analyzed by next generation sequencing. (C and D) Percentage of deletion patterns in HPCs and LSECs after treatment of Cas9/NSGHAsgRNA LNPs are shown. Data are presented as average experimental values ±standard deviation.

of tumorigenesis.[57–63] In addition to integrative lentiviral vectors, there is increasing evidence that AAV vectors can also integrate into the host genomic DNA at a low frequency following transduction in various animal models, including mice,[57,58] dogs,[59,60] non-human primates,[61–63] and humans.[62]

Furthermore, gene editing results in the biosynthesis of full-length FVIII at its natural site. In contrast, most gene transfer therapies including AAV and lentivirus-based therapy employ vectors expressing B-domain deleted (BDD) FVIII, which poses challenges in folding and secretion.[64] The accumulation of BDD FVIII protein may exceed hepatocytes' capacity for proper folding and secretion, leading to an increase in ER stress both *in vitro and in vivo*.[25,65,66] Additionally, the accumulation of misfolded BDD FVIII in the ER can trigger cytotoxic responses and potentially contribute to tumorigenesis when subjected to a high-fat diet (HFD). These findings highlight the importance of careful consideration for gene transfer of BDD FVIII.[67,68] Although we showed that delivery of CRISPR-based gene editing tools by LNPs also produced a high rate of gene correction in hepatocytes, it does not result in functional ectopic FVIII expression, which, if present, could potentially cause cellular toxicity. However, it neither impacted functional FVIII expression in LSECs nor induced any toxicity in mice.

Targeted gene delivery and editing specifically aimed at LSECs hold significant promise for addressing changes related to LSECs in liver diseases. In physiological conditions, LSECs regulate hepatic vascular tone and maintain the quiescence of hepatic stellate cells, thereby preventing intrahepatic vasoconstriction and fibrosis. In pathological states, LSECs are pivotal in the initiation and progression of chronic liver diseases and hepatocellular carcinoma. Moreover, LSECs play crucial roles in aging, inflammation, and infection.[69] Increasing evidence underscores the growing importance of LSEC-targeting therapeutics. Protecting LSECs from apoptosis not only mitigates hepatocyte apoptosis but also effectively treats acute liver failure. Previous studies have shown that the delivery of Bax siRNA can inhibit LSEC apoptosis, while LOX-1 siRNA delivery can reduce fenestration diameter and porosity in LSECs, which are phenomena associated with the progression of aging-related diseases and LSEC dysfunction.[70,71]

In conclusion, the gene correction of mutant *F8* to rescue endogenous FVIII expression using Cas9 mRNA LNP offers several significant advantages. LNPs as therapeutic delivery vehicles are suitable for most HemA patients without the need for screening for antibodies against viral vectors. The use of target-specific Cas9 protein allows for the identification and prevention of off-target effects. Furthermore,

transient expression of Cas9 protein through Cas9 mRNA further reduces the risk of off-target events. Moreover, the rescued endogenous FVIII protein can be stored and released via physiological pathways in a controlled manner, avoiding misfolding issues associated with BDD FVIII and reducing ER stress. To further enhance gene editing efficiency, incorporating base editing or prime editing tools with LNP technology holds great promise for expanding the range of *F8* gene corrections, including missense, nonsense, and frameshift variants in HemA patients. This avenue of research represents the next step in advancing precision gene therapy for HemA, offering the potential for more comprehensive and effective treatments.

## MATERIALS AND METHODS

### Reagent

Luciferase, GFP, and Cas9 mRNA were purchased from TriLink Biotechnologies (San Diego, CA, USA) or GeneScript (Piscataway, NJ, USA). mF8sgRNA and NSGHAsgRNA were purchased from Integrated DNA Technologies (San Diego, CA, USA). 1,2-dioleoyl-sn-glycero-3-phosphoethanolamine (DOPE), 1,2-dimyristoyl-rac-glycero-3-methoxypolyethylene glycol-2000 (DMG-PEG2K), and cholesterol were purchased from Avanti Polar Lipids (Alabaster, USA). D-Lin-MC3-DMA (MC3) was purchased from Chemscene (Monmouth Junction, NJ, USA) or MedKoo (Morrisville, NJ, USA). Antibodies against GFP (A10262, Thermo Scientific, WA, USA), CD31 (102510, BioLegend, San Diego, CA, USA), CD45 (103133, BioLegend, USA), CD146 (130-118-407, Miltenyi Biotec, USA), and LYVE-1 (AF2125, R&D Systems, MN, USA). 1,1′-Dioctadecyl-3,3,3′,3′-tetramethylindocarbocyanine perchlorate (DiI) was purchased from Sigma-Aldrich. Fluorescein Griffonia Simplicifolia Lectin I Isolectin B4 (Fluorescein-IB4, FL-1201-.5) was purchased from Vector Laboratories (Newark, NJ, USA). T7 endonuclease I was purchased from New England Biolabs (M0302S).

### Synthesis of LNP

All the lipid components (MC3:DOPE:cholesterol:DMG-PEG2K = 50:10:39:1) were dissolved in ethanol. mRNAs were diluted in 50-mM sodium citrate buffer (pH = 3). Organic and aqueous solutions were assembled using NanoAssemblr system (Precision NanoSystems, San Francisco, CA, USA) at a 1:3 volume ratio to synthesize mRNA LNPs. Encapsulation efficiency of mRNA LNPs was determined by Quant-it RiboGreen RNA Assay Kit (Thermo Fisher, USA). The particle size distribution and average size were measured using the qNano instrument with an NP200 membrane (Izon Science, NZ).

### Animal

HemA mice with disruption of FVIII exon 16 were used in 129/SV × C57BL/6 mixed genetic background. NOD.Cg-Prkdc$^{scid}$ Il2rg$^{tm1Wjl}$/SzJ mice (NSG mice) were purchased from Jackson Laboratory (Sacramento, CA, USA). NSG HemA mice were purchased from Gene Knockout Mouse Core Facility of NTU Center of Genomic and Precision Medicine (Taipei, Taiwan). All the experimental mice were housed at a specific pathogen-free (SPF) facility in Seattle Children's Research Institute according to the animal care guidelines of National Institutes of Health and Seattle Children's

Research Institute. The experimental protocols used in this study were approved by the Institutional Animal Care and Use Committee of Seattle Children's Research Institute.

### T7E1 assay

NIH3T3cells were transfected with Cas9 protein (1081059, IDT) and two sgRNAs using CRISPRMax (Invitrogen, CA, USA), respectively. At 72 h post-transfection, genomic DNA was extracted from transfected cells using DNeasy Blood & Tissue Kit (Qiagen). The mouse FVIII region targeted by sgRNA was amplified using CloneAmp HiFi PCR Premix (Takara Bio, USA) with primers mF8-VF1: 5′-TGCTCTGCAAAATATTTAGGACT-3′ and mF8-VR1: 5′-TTA CACTAAGAAACACCTAGTAG-3′ yielding a PCR fragment of 426 base pairs in WT mouse FVIII and 421 base pairs in mutant FVIII, respectively. PCR fragments were purified using NucleoSpin Gel and PCR Clean-Up kit (Takara) and quantified using a Nanodrop Spectrophotometer (Nanodrop One, Thermo Fischer, USA). For the T7E1 assay, 100 ng of PCR products were heated, following cooling down to room temperature as follows: 95°C for 5 min, from 95°C to 85°C at − 2°C per second, from 85°C to 25°C at − 0.1°C per second. After heteroduplex formation, 10 units of T7E1 enzyme (New England Biolabs, USA) were added to the samples and incubated at 37°C for 15 min. PCR fragments were analyzed by gel electrophoresis. The gene editing rate was estimated according to the following formula:

$$\frac{\text{Amount of digested products}}{\text{Total amount of digested products and undigested parental band}} \times 100\%$$

### LNP injection and samples collection

Different mRNA LNPs were intravenously injected to mice through retro-orbital plexus. Blood samples were collected from retro-orbital plexus and centrifuged immediately to obtain sera. Samples were stored at −80°C for further experiments.

### Live imaging of experimental mice using an intravital imaging system

Mice were subcutaneously injected with 200 μL/20 g of D-Luciferin (PI88293, Fisher Scientific) 10 min before imaging. All the images were monitored by Image Studio Software for Pearl Trilogy Imaging System (LI-COR, USA).

### Immunofluorescent staining and flow cytometry

Mouse livers were harvested, fixed in 4% paraformaldehyde (RT-15710, Electron Microscopy Sciences, PA, USA) for 1 h at room temperature and cryoprotected in PBS (phosphate-buffered saline) with 30% sucrose at 4°C overnight. Liver sections were blocked in 0.5% fetal bovine serum in PBS and stained with anti-GFP (A10262, Thermo Scientific, WA, USA), CD31 (14-0311-81, Thermo Scientific) and LYVE-1 (AF2125, R&D Systems, MN, USA) at 4°C overnight, followed by application of the secondary antibodies conjugated with Alexa Fluor 488 or 594 (Invitrogen). For vascular staining, PBS containing 20 μg/mL Isolectin GS-IB4 (I21411, Thermo Scientific) with Alexa Fluor 488 conjugate was

added to sections and stained at room temperature for 2 h. Sections were mounted with mounting medium containing DAPI (H-1200-10, Vector Laboratories, CA, USA) for nuclear staining. Images were examined on a fluorescent microscope (DM6000B, Lecia). To verify cell-type-specific gene editing, the livers of treated mice were perfused with HBSS buffer containing 0.5 mM EDTA and 25 mM HEPES, followed by digestion with a buffer containing Liberase (5401119001, Sigma-Aldrich). Hepatocytes were isolated by centrifugation at $50 \times g$ for 2 min. LSECs were further isolated using mouse CD146 MicroBeads (130-092-007, Miltenyi Biotec). The isolated cells were stained with APC-labeled anti-CD31, (102510, BioLegend), BV421-labeled, anti-CD45 (103133, BioLegend), and PE-labeled anti-CD146 (130-118-407, Miltenyi Biotec). Finally, the labeled cells were analyzed using an LSRFortessa (BD Biosciences) or CytoFLEX (Beckman Coulter) flow cytometer.

### In vitro luciferase assay

Liver lobes were homogenized using Bead Ruptor Elite (OMNI, US) in passive lysis buffer (E1941, Promega, USA). Total protein of isolated hepatocytes and LSECs were directly extracted using passive lysis buffer. Luciferase activity in the extracted protein fraction was evaluated by Luciferase Assay System (Promega) and measured by a Victor 3 plate reader (PerkinElmer, USA). Luciferase expression was normalized by total protein, measured by BCA assay kit (Bio-Rad, USA), and reported as RLU/mg.

### aPTT assay

Plasma mouse FVIII was examined using activated partial thromboplastin time (aPTT) assay.[16,55] Mouse FVIII activity was evaluated according to a standard curve obtained from serially diluted normal human pooled plasma.

### AST and ALT assays

Liver injury was evaluated using alanine aminotransferase (ALT) reagent kit (Teco diagnostics, Anaheim, CA) and aspartate aminotransferase (AST) commercial enzyme kit (Randox, London, United Kingdom) at indicated time points after LNP injection, respectively.

### Hydrodynamic injection

For the hydrodynamic injection of sgRNA and Cas9 plasmids, we incorporated mF8sgRNA and NSGHAsgRNA, respectively into the pL-CRISPR.EFS.tRFP plasmid (a gift from Benjamin Ebert, Addgene plasmid # 57819; http://n2t.net/addgene:57819; RRID: Addgene_57819). These constructs were hydrodynamically injected into NSG HemA mice at a concentration of 50 μg/mL and a volume (mL) equal to 9% the mouse's body weight (g). Blood samples were collected weekly via retro-orbital bleeding, with one-tenth volume of 3.8% sodium citrate added to each sample. A second hydrodynamic injection was performed in week 5, and blood samples were collected weekly up to week 10.

### Thromboelastography

Coagulation function of experimental mice treated with Cas9 mRNA LNPs was examined at indicated time points after treatment. Un-

treated NSG HemA mice were served as control. Whole blood was collected by submental bleeding and mixed with anticoagulant 3.8% citric acid at a ratio of 1:9 (anticoagulant: whole blood). CT and CFT were directly measured using NATEM (Non-Activated Thromboelastometry) kit assay by rotational thromboelastometry (ROTEM delta, Instrumentation Laboratory, Bedford, MA).

### Sanger sequencing and deep sequencing

Genomic DNA of treated mice was extracted from transfected cells using DNeasy Blood & Tissue Kit (Qiagen) at indicated time points. The mouse FVIII region targeted by sgRNA was amplified using CloneAmp HiFi PCR Premix (Takara Bio) with primers mF8-VF1 and mF8-VR1. PCR fragments were purified using NucleoSpin Gel and PCR Clean-Up kit (Takara) and quantified using Nanodrop Spectrophotometer. To identify the gene editing rate, purified PCR amplicons were shipped to Azenta Life Sciences (Seattle, WA, USA) for Sanger sequencing or deep sequencing. The Sanger sequencing data were analyzed using Tracking of indels by Decomposition (TIDE) (http://shinyapps.datacurators.nl/tide/) or Synthego ICE analysis (https://ice.synthego.com/#/). Next generation sequencing (NGS) data were analyzed by Azenta or Cas-Analyzer (Rgen tool, http://www.rgenome.net/cas-analyzer/#!).

### Statistical analyses

All the statistical analyses were carried out utilizing GraphPad Prism 7 software. The data were compared using two-tailed unpaired Student's t test and one-way analysis of variance (ANOVA) followed by post hoc Bonferroni's multiple comparison tests; $p$ values <0.05 were considered statistically significant.

## DATA AND CODE AVAILABILITY

The data that support the findings of this study are available on request from the corresponding author Carol Miao, carol.miao@seattlechildrens.org.

## AUTHOR CONTRIBUTIONS

C.-Y.C. developed study design, performed experiments, analyzed data, and wrote and revised the manuscript. X.C. performed aPTT experiments. C.H.M. developed the study concept, analyzed results, and wrote and revised the manuscript.

## DECLARATION OF INTERESTS

C.H.M. is an editorial board member of Molecular Therapy and has a patent application related to this work.

## SUPPLEMENTAL INFORMATION

Supplemental information can be found online at https://doi.org/10.1016/j.omtn.2024.102383.

## REFERENCES

1. Davie, E.W., Fujikawa, K., and Kisiel, W. (1991). The coagulation cascade: initiation, maintenance, and regulation. Biochemistry 30, 10363–10370.

2. Sarmiento Doncel, S., Díaz Mosquera, G.A., Cortes, J.M., Agudelo Rico, C., Meza Cadavid, F.J., and Peláez, R.G. (2023). Haemophilia A: A Review of Clinical

Manifestations, Treatment, Mutations, and the Development of Inhibitors. Hematol. Rep. *15*, 130–150.

3. Samelson-Jones, B.J., and George, L.A. (2023). Adeno-Associated Virus Gene Therapy for Hemophilia. Annu. Rev. Med. *74*, 231–247.

4. Pipe, S.W., Arruda, V.R., Lange, C., Kitchen, S., Eichler, H., and Wadsworth, S. (2023). Characteristics of BAY 2599023 in the Current Treatment Landscape of Hemophilia A Gene Therapy. Curr. Gene Ther. *23*, 81–95.

5. Zhou, L., and Yao, S. (2023). Recent advances in therapeutic CRISPR-Cas9 genome editing: mechanisms and applications. Mol. Biomed. *4*, 10.

6. Bennett, E.P., Petersen, B.L., Johansen, I.E., Niu, Y., Yang, Z., Chamberlain, C.A., Met, Ö., Wandall, H.H., and Frödin, M. (2020). INDEL detection, the 'Achilles heel' of precise genome editing: a survey of methods for accurate profiling of gene editing induced indels. Nucleic Acids Res. *48*, 11958–11981.

7. Samaridou, E., Heyes, J., and Lutwyche, P. (2020). Lipid nanoparticles for nucleic acid delivery: Current perspectives. Adv. Drug Deliv. Rev. *154–155*, 37–63.

8. Cullis, P.R., and Hope, M.J. (2017). Lipid Nanoparticle Systems for Enabling Gene Therapies. Mol. Ther. *25*, 1467–1475.

9. Wang, Z., Ma, W., Fu, X., Qi, Y., Zhao, Y., and Zhang, S. (2023). Development and applications of mRNA treatment based on lipid nanoparticles. Biotechnol. Adv. *65*, 108130.

10. Akinc, A., Maier, M.A., Manoharan, M., Fitzgerald, K., Jayaraman, M., Barros, S., Ansell, S., Du, X., Hope, M.J., Madden, T.D., et al. (2019). The Onpattro story and the clinical translation of nanomedicines containing nucleic acid-based drugs. Nat. Nanotechnol. *14*, 1084–1087.

11. Urits, I., Swanson, D., Swett, M.C., Patel, A., Berardino, K., Amgalan, A., Berger, A.A., Kassem, H., Kaye, A.D., and Viswanath, O. (2020). A Review of Patisiran (ONPATTRO(R)) for the Treatment of Polyneuropathy in People with Hereditary Transthyretin Amyloidosis. Neurol. Ther. *9*, 301–315.

12. Hogan, M.J., and Pardi, N. (2022). mRNA Vaccines in the COVID-19 Pandemic and Beyond. Annu. Rev. Med. *73*, 17–39.

13. Schoenmaker, L., Witzigmann, D., Kulkarni, J.A., Verbeke, R., Kersten, G., Jiskoot, W., and Crommelin, D.J.A. (2021). mRNA-lipid nanoparticle COVID-19 vaccines: Structure and stability. Int. J. Pharm. *601*, 120586.

14. Sebastiani, F., Yanez Arteta, M., Lerche, M., Porcar, L., Lang, C., Bragg, R.A., Elmore, C.S., Krishnamurthy, V.R., Russell, R.A., Darwish, T., et al. (2021). Apolipoprotein E Binding Drives Structural and Compositional Rearrangement of mRNA-Containing Lipid Nanoparticles. ACS Nano *15*, 6709–6722.

15. Akinc, A., Querbes, W., De, S., Qin, J., Frank-Kamenetsky, M., Jayaprakash, K.N., Jayaraman, M., Rajeev, K.G., Cantley, W.L., Dorkin, J.R., et al. (2010). Targeted delivery of RNAi therapeutics with endogenous and exogenous ligand-based mechanisms. Mol. Ther. *18*, 1357–1364.

16. Chen, C.Y., Tran, D.M., Cavedon, A., Cai, X., Rajendran, R., Lyle, M.J., Martini, P.G.V., and Miao, C.H. (2020). Treatment of Hemophilia A Using Factor VIII Messenger RNA Lipid Nanoparticles. Mol. Ther. Nucleic Acids *20*, 534–544.

17. Chen, C.Y., Vander Kooi, A., Cavedon, A., Cai, X., Hoggatt, J., Martini, P.G.V., and Miao, C.H. (2023). Induction of long-term tolerance to a specific antigen using anti-CD3 lipid nanoparticles following gene therapy. Mol. Ther. Nucleic Acids *34*, 102043.

18. Do, H., Healey, J.F., Waller, E.K., and Lollar, P. (1999). Expression of factor VIII by murine liver sinusoidal endothelial cells. J. Biol. Chem. *274*, 19587–19592.

19. Terada, T., Kulkarni, J.A., Huynh, A., Tam, Y.Y.C., and Cullis, P. (2021). Protective Effect of Edaravone against Cationic Lipid-Mediated Oxidative Stress and Apoptosis. Biol. Pharm. Bull. *44*, 144–149.

20. Cui, S., Wang, Y., Gong, Y., Lin, X., Zhao, Y., Zhi, D., Zhou, Q., and Zhang, S. (2018). Correlation of the cytotoxic effects of cationic lipids with their headgroups. Toxicol. Res. *7*, 473–479.

21. Sun, D., and Lu, Z.R. (2023). Structure and Function of Cationic and Ionizable Lipids for Nucleic Acid Delivery. Pharm. Res. (N. Y.) *40*, 27–46.

22. Sago, C.D., Krupczak, B.R., Lokugamage, M.P., Gan, Z., and Dahlman, J.E. (2019). Cell Subtypes Within the Liver Microenvironment Differentially Interact with Lipid Nanoparticles. Cell. Mol. Bioeng. *12*, 389–397.

23. Gary, D.J., Min, J., Kim, Y., Park, K., and Won, Y.Y. (2013). The effect of N/P ratio on the in vitro and in vivo interaction properties of PEGylated poly[2-(dimethylamino) ethyl methacrylate]-based siRNA complexes. Macromol. Biosci. *13*, 1059–1071.

24. Algarni, A., Pilkington, E.H., Suys, E.J.A., Al-Wassiti, H., Pouton, C.W., and Truong, N.P. (2022). In vivo delivery of plasmid DNA by lipid nanoparticles: the influence of ionizable cationic lipids on organ-selective gene expression. Biomater. Sci. *10*, 2940–2952.

25. Fong, S., Handyside, B., Sihn, C.R., Liu, S., Zhang, L., Xie, L., Murphy, R., Galicia, N., Yates, B., Minto, W.C., et al. (2020). Induction of ER Stress by an AAV5 BDD FVIII Construct Is Dependent on the Strength of the Hepatic-Specific Promoter. Mol. Ther. Methods Clin. Dev. *18*, 620–630.

26. Han, X., Gong, N., Xue, L., Billingsley, M.M., El-Mayta, R., Shepherd, S.J., Alameh, M.G., Weissman, D., and Mitchell, M.J. (2023). Ligand-tethered lipid nanoparticles for targeted RNA delivery to treat liver fibrosis. Nat. Commun. *14*, 75.

27. Yin, H., Song, C.Q., Dorkin, J.R., Zhu, L.J., Li, Y., Wu, Q., Park, A., Yang, J., Suresh, S., Bizhanova, A., et al. (2016). Therapeutic genome editing by combined viral and non-viral delivery of CRISPR system components in vivo. Nat. Biotechnol. *34*, 328–333.

28. Song, C.Q., Jiang, T., Richter, M., Rhym, L.H., Koblan, L.W., Zafra, M.P., Schatoff, E.M., Doman, J.L., Cao, Y., Dow, L.E., et al. (2020). Adenine base editing in an adult mouse model of tyrosinaemia. Nat. Biomed. Eng. *4*, 125–130.

29. Castaman, G., and Matino, D. (2019). Hemophilia A and B: molecular and clinical similarities and differences. Haematologica *104*, 1702–1709.

30. Begbie, M., Notley, C., Tinlin, S., Sawyer, L., and Lillicrap, D. (2000). The Factor VIII acute phase response requires the participation of NFkappaB and C/EBP. Thromb. Haemost. *84*, 216–222.

31. Collins, P.W., Macchiavello, L.I., Lewis, S.J., Macartney, N.J., Saayman, A.G., Luddington, R., Baglin, T., and Findlay, G.P. (2006). Global tests of haemostasis in critically ill patients with severe sepsis syndrome compared to controls. Br. J. Haematol. *135*, 220–227.

32. Tanaka, K.A., Bharadwaj, S., Hasan, S., Judd, M., Abuelkasem, E., Henderson, R.A., Chow, J.H., Williams, B., Mazzeffi, M.A., Crimmins, S.D., and Malinow, A.M. (2019). Elevated fibrinogen, von Willebrand factor, and Factor VIII confer resistance to dilutional coagulopathy and activated protein C in normal pregnant women. Br. J. Anaesth. *122*, 751–759.

33. Tabatabai, A., Rabin, J., Menaker, J., Madathil, R., Galvagno, S., Menne, A., Chow, J.H., Grazioli, A., Herr, D., Tanaka, K., et al. (2020). Factor VIII and Functional Protein C Activity in Critically Ill Patients With Coronavirus Disease 2019: A Case Series. A. A. Pract. *14*, e01236.

34. Arai, M., Yorifuji, H., Ikematsu, S., Nagasawa, H., Fujimaki, M., Fukutake, K., Katsumura, T., Ishii, T., and Iwane, H. (1990). Influences of strenuous exercise (triathlon) on blood coagulation and fibrinolytic system. Thromb. Res. *57*, 465–471.

35. Lin, X., El-Sayed, M.S., Waterhouse, J., and Reilly, T. (1999). Activation and disturbance of blood haemostasis following strenuous physical exercise. Int. J. Sports Med. *20*, 149–153.

36. Beltrame, L.G.N., Abreu, L., Almeida, J., and Boullosa, D.A. (2015). The acute effect of moderate intensity aquatic exercise on coagulation factors in haemophiliacs. Clin. Physiol. Funct. Imaging *35*, 191–196.

37. Kumar, R., Bouskill, V., Schneiderman, J.E., Pluthero, F.G., Kahr, W.H.A., Craik, A., Clark, D., Whitney, K., Zhang, C., Rand, M.L., and Carcao, M. (2016). Impact of aerobic exercise on haemostatic indices in paediatric patients with haemophilia. Thromb. Haemost. *115*, 1120–1128.

38. Hayakawa, M., Sakata, A., Hayakawa, H., Matsumoto, H., Hiramoto, T., Kashiwakura, Y., Baatartsogt, N., Fukushima, N., Sakata, Y., Suzuki-Inoue, K., and Ohmori, T. (2021). Characterization and visualization of murine coagulation factor VIII-producing cells in vivo. Sci. Rep. *11*, 14824.

39. Pierce, G.F., and Mattis, A.N. (2022). Transient expression of factor VIII and a chronic high-fat diet induces ER stress and late hepatocyte oncogenesis. Mol. Ther. *30*, 3510–3512.

40. Fong, S., Yates, B., Sihn, C.R., Mattis, A.N., Mitchell, N., Liu, S., Russell, C.B., Kim, B., Lawal, A., Rangarajan, S., et al. (2022). Interindividual variability in transgene mRNA and protein production following adeno-associated virus gene therapy for hemophilia A. Nat. Med. *28*, 789–797.

41. Lenting, P.J., van Mourik, J.A., and Mertens, K. (1998). The life cycle of coagulation factor VIII in view of its structure and function. Blood *92*, 3983–3996.

42. Pan, J., Dinh, T.T., Rajaraman, A., Lee, M., Scholz, A., Czupalla, C.J., Kiefel, H., Zhu, L., Xia, L., Morser, J., et al. (2016). Patterns of expression of factor VIII and von Willebrand factor by endothelial cell subsets in vivo. Blood *128*, 104–109.

43. Rosenberg, J.B., Foster, P.A., Kaufman, R.J., Vokac, E.A., Moussalli, M., Kroner, P.A., and Montgomery, R.R. (1998). Intracellular trafficking of factor VIII to von Willebrand factor storage granules. J. Clin. Invest. *101*, 613–624.

44. Shi, Q., Schroeder, J.A., Kuether, E.L., and Montgomery, R.R. (2015). The important role of von Willebrand factor in platelet-derived FVIII gene therapy for murine hemophilia A in the presence of inhibitory antibodies. J. Thromb. Haemost. *13*, 1301–1309.

45. Rosenberg, J.B., Greengard, J.S., and Montgomery, R.R. (2000). Genetic induction of a releasable pool of factor VIII in human endothelial cells. Arterioscler. Thromb. Vasc. Biol. *20*, 2689–2695.

46. van den Biggelaar, M., Bouwens, E.A.M., Voorberg, J., and Mertens, K. (2011). Storage of factor VIII variants with impaired von Willebrand factor binding in Weibel-Palade bodies in endothelial cells. PLoS One *6*, e24163.

47. Turner, N.A., and Moake, J.L. (2015). Factor VIII Is Synthesized in Human Endothelial Cells, Packaged in Weibel-Palade Bodies and Secreted Bound to ULVWF Strings. PLoS One *10*, e0140740.

48. Diehl, L., Schurich, A., Grochtmann, R., Hegenbarth, S., Chen, L., and Knolle, P.A. (2008). Tolerogenic maturation of liver sinusoidal endothelial cells promotes B7-homolog 1-dependent CD8+ T cell tolerance. Hepatology *47*, 296–305.

49. Carambia, A., Freund, B., Schwinge, D., Heine, M., Laschtowitz, A., Huber, S., Wraith, D.C., Korn, T., Schramm, C., Lohse, A.W., et al. (2014). TGF-beta-dependent induction of CD4(+)CD25(+)Foxp3(+) Tregs by liver sinusoidal endothelial cells. J. Hepatol. *61*, 594–599.

50. Kruse, N., Neumann, K., Schrage, A., Derkow, K., Schott, E., Erben, U., Kühl, A., Loddenkemper, C., Zeitz, M., Hamann, A., and Klugewitz, K. (2009). Priming of CD4+ T cells by liver sinusoidal endothelial cells induces CD25low forkhead box protein 3- regulatory T cells suppressing autoimmune hepatitis. Hepatology *50*, 1904–1913.

51. Merlin, S., Cannizzo, E.S., Borroni, E., Bruscaggin, V., Schinco, P., Tulalamba, W., Chuah, M.K., Arruda, V.R., VandenDriessche, T., Prat, M., et al. (2017). A Novel Platform for Immune Tolerance Induction in Hemophilia A Mice. Mol. Ther. *25*, 1815–1830.

52. Merlin, S., Famà, R., Borroni, E., Zanolini, D., Bruscaggin, V., Zucchelli, S., and Follenzi, A. (2019). FVIII expression by its native promoter sustains long-term correction avoiding immune response in hemophilic mice. Blood Adv. *3*, 825–838.

53. Mahlangu, J., Kaczmarek, R., von Drygalski, A., Shapiro, S., Chou, S.C., Ozelo, M.C., Kenet, G., Peyvandi, F., Wang, M., Madan, B., et al. (2023). Two-Year Outcomes of Valoctocogene Roxaparvovec Therapy for Hemophilia A. N. Engl. J. Med. *388*, 694–705.

54. Bolous, N.S., Bhatt, N., Bhakta, N., Neufeld, E.J., Davidoff, A.M., and Reiss, U.M. (2022). Gene Therapy and Hemophilia: Where Do We Go from Here? J. Blood Med. *13*, 559–580.

55. Chen, C.Y., Kooi, A.V., Cavedon, A., Cai, X.H., Hoggatt, J., Martini, P.G.V., and Miao, C.H. (2023). Induction of long-term tolerance to a specific antigen using anti-CD3 lipid nanoparticles following gene therapy. Mol Ther Nucl Acids *34*, 102043.

56. Kenjo, E., Hozumi, H., Makita, Y., Iwabuchi, K.A., Fujimoto, N., Matsumoto, S., Kimura, M., Amano, Y., Ifuku, M., Naoe, Y., et al. (2021). Low immunogenicity of LNP allows repeated administrations of CRISPR-Cas9 mRNA into skeletal muscle in mice. Nat. Commun. *12*, 7101.

57. Zhong, L., Malani, N., Li, M., Brady, T., Xie, J., Bell, P., Li, S., Jones, H., Wilson, J.M., Flotte, T.R., et al. (2013). Recombinant adeno-associated virus integration sites in murine liver after ornithine transcarbamylase gene correction. Hum. Gene Ther. *24*, 520–525.

58. Li, H., Malani, N., Hamilton, S.R., Schlachterman, A., Bussadori, G., Edmonson, S.E., Shah, R., Arruda, V.R., Mingozzi, F., Wright, J.F., et al. (2011). Assessing the potential for AAV vector genotoxicity in a murine model. Blood *117*, 3311–3319.

59. Nguyen, G.N., Everett, J.K., Kafle, S., Roche, A.M., Raymond, H.E., Leiby, J., Wood, C., Assenmacher, C.A., Merricks, E.P., Long, C.T., et al. (2021). A long-term study of AAV gene therapy in dogs with hemophilia A identifies clonal expansions of transduced liver cells. Nat. Biotechnol. *39*, 47–55.

60. Mattar, C.N.Z., Gil-Farina, I., Rosales, C., Johana, N., Tan, Y.Y.W., McIntosh, J., Kaeppel, C., Waddington, S.N., Biswas, A., Choolani, M., et al. (2017). In Utero Transfer of Adeno-Associated Viral Vectors Produces Long-Term Factor IX Levels in a Cynomolgus Macaque Model. Mol. Ther. *25*, 1843–1853.

61. Nowrouzi, A., Penaud-Budloo, M., Kaeppel, C., Appelt, U., Le Guiner, C., Moullier, P., von Kalle, C., Snyder, R.O., and Schmidt, M. (2012). Integration Frequency and Intermolecular Recombination of rAAV Vectors in Non-human Primate Skeletal Muscle and Liver. Mol. Ther. *20*, 1177–1186.

62. Gil-Farina, I., Fronza, R., Kaeppel, C., Lopez-Franco, E., Ferreira, V., D'Avola, D., Benito, A., Prieto, J., Petry, H., Gonzalez-Aseguinolaza, G., and Schmidt, M. (2016). Recombinant AAV Integration Is Not Associated With Hepatic Genotoxicity in Nonhuman Primates and Patients. Mol. Ther. *24*, 1100–1105.

63. Breton, C., Clark, P.M., Wang, L., Greig, J.A., and Wilson, J.M. (2020). ITR-Seq, a next-generation sequencing assay, identifies genome-wide DNA editing sites in vivo following adeno-associated viral vector-mediated genome editing. BMC Genom. *21*, 239.

64. Miao, H.Z., Sirachainan, N., Palmer, L., Kucab, P., Cunningham, M.A., Kaufman, R.J., and Pipe, S.W. (2004). Bioengineering of coagulation factor VIII for improved secretion. Blood *103*, 3412–3419.

65. Zolotukhin, I., Markusic, D.M., Palaschak, B., Hoffman, B.E., Srikanthan, M.A., and Herzog, R.W. (2016). Potential for cellular stress response to hepatic factor VIII expression from AAV vector. Mol. Ther. Methods Clin. Dev. *3*, 16063.

66. Lange, A.M., Altynova, E.S., Nguyen, G.N., and Sabatino, D.E. (2016). Overexpression of factor VIII after AAV delivery is transiently associated with cellular stress in hemophilia A mice. Mol. Ther. Methods Clin. Dev. *3*, 16064.

67. Zhao, J., Zhou, M., Wang, Z., Wu, L., Hu, Z., and Liang, D. (2022). Ectopic Expression of FVIII in HPCs and MSCs Derived from hiPSCs with Site-Specific Integration of ITGA2B Promoter-Driven BDDF8 Gene in Hemophilia A. Int. J. Mol. Sci. *23*, 623.

68. Dalwadi, D.A., Torrens, L., Abril-Fornaguera, J., Pinyol, R., Willoughby, C., Posey, J., Llovet, J.M., Lanciault, C., Russell, D.W., Grompe, M., and Naugler, W.E. (2021). Liver Injury Increases the Incidence of HCC following AAV Gene Therapy in Mice. Mol. Ther. *29*, 680–690.

69. Poisson, J., Lemoinne, S., Boulanger, C., Durand, F., Moreau, R., Valla, D., and Rautou, P.E. (2017). Liver sinusoidal endothelial cells: Physiology and role in liver diseases. J. Hepatol. *66*, 212–227.

70. Tanoi, T., Tamura, T., Sano, N., Nakayama, K., Fukunaga, K., Zheng, Y.W., Akhter, A., Sakurai, Y., Hayashi, Y., Harashima, H., and Ohkohchi, N. (2016). Protecting liver sinusoidal endothelial cells suppresses apoptosis in acute liver damage. Hepatol. Res. *46*, 697–706.

71. Pandey, E., Nour, A.S., and Harris, E.N. (2020). Prominent Receptors of Liver Sinusoidal Endothelial Cells in Liver Homeostasis and Disease. Front. Physiol. *11*, 873.